Approved for public release; distribution is unlimited.

Unified Data Fusion Applied to Monopulse Tracking[1]

25 May 1999

Michael V. Finn
Metron, Incorporated
11911 Freedom Drive, Suite 800
Reston, VA 20190-5602
(703)-787-8700

Abstract

The direction of arrival (DOA) computed from the monopulse ratio is known to fluctuate widely in the presence of multiple unresolved targets. This confounds traditional trackers operating on unresolved targets, leading to erroneous state estimates or loss of track. This paper presents a computationally feasible solution to this problem using Metron's Unified Theory of Data Fusion (UDF). UDF is a Bayesian method that maintains a probability density on the joint target state space. It operates without explicitly enumerating multiple data-to-target associations. This is particularly important for unresolved targets where the data cannot be attributed to a single target. Likelihood functions for two Rayleigh targets over a range of SNRs are examined first to develop insight. The final example presents the application to tracking two low-SNR targets crossing the radar beam.

1. Introduction

The monopulse technique is designed to provide precise angular measurements of a target's location. (See reference [5].) The monopulse system sends out a single pulse and then receives on two beams offset (squinted) relative to the transmit pulse axis. More power received in the right beam than the left beam indicates that the target is likely on the right side of the transmit beam. Similarly, if the left beam's return is larger, the target is likely to the left. The magnitude of the difference gives an indication of how far the target is off axis. With a single

[1] This work was performed under contract N00014-95-C-0052 to the Office of Naval Research.

transmit pulse, pulse-to-pulse fluctuations in reflected energy—which degrade scanning techniques—are not detrimental. The monopulse system requires two squinted beams for azimuth and two for elevation. In the examples shown below we will be working with one coordinate, and assume that the other coordinate may be tracked independently. Monopulse

processing is not strictly a radar technique; it can be used to track emissions passively and has also been suggested as a means to improve sonar tracking with a linear array ([4]).

Unresolved targets cause problems for monopulse trackers. The standard processor assumes that the response is due to a single target. When two targets are present—or a target and a jammer, or a single large target with multiple scattering centers, or two apparent targets due to multipath—the monopulse ratio may wander beyond the angular separation of the targets, causing loss of track. Detecting the presence of unresolved targets has attracted interest from a number of researchers. However the tracking aspect has only recently been addressed by Blair and Brandt-Pearce ([3]). They use estimates of the first two moments of the monopulse ratio derived from a small number of pulses are used to extract estimates of the Directions of Arrival (DOAs). These estimates (along with covariance estimates) were used in a simulation of two targets under track converging to the point of being unresolved by the radar. The simulations showed that without multi-target processing the tracks were lost in every simulation. With multi-target processing the tracks were maintained, but there was a strong bias in the state estimates toward the radar axis. They concluded that: “Further investigations are needed so that the bias in the estimates can be reduced and the transition from tracking resolved targets and unresolved targets can be improved.” This paper demonstrates how Unified Data Fusion may naturally be applied to solving this problem.

The theoretical basis of UDF has been presented in references [1] and [6]. Briefly stated, UDF approaches the multiple target tracking problem by working in the joint state space of the possible targets. If the number of targets is unknown (as in the examples to be presented below), then the full state space is the union of *n*-target state spaces. All data pertaining to the targets is contained in a probability distribution over the joint state space. The distribution is updated through two processes: information updating to incorporate new data, and motion updating to model the targets’ mobility during time periods when no new data arrives. UDF computes the true Bayesian posterior on the joint state space. It can handle nonlinear motion, nonGaussian state distributions, nonGaussian measurement error models, and nonlinear relationships between state and measurement. The price of such generality is that the state space can become quite large for problems involving many targets. Examples in [1] and [6] worked with simplified two-target scenarios in order to illustrate concepts. The application presented here also involves two targets, but the power of UDF to handle the full complexity of the problem produces results superior to other approaches.

The paper is organized as follows. The second section reviews the monopulse problem and introduces some notation. The third section identifies the key statistical properties needed for UDF. The fourth section describes how UDF is applied to the monopulse problem and the

parameters used in the simulation. The fifth section presents a number of examples of typical likelihood functions and discusses their properties. The sixth section presents results of a simulation where two unresolved targets are tracked. The last section a summary.

2. Notation

We will use reference [2] for our notation. A radar dwell is composed of a small number of pulses; in the examples that follow we have 6 pulses. The data to be fused consists of the in-phase and quadrature signals in the sum and difference channels which we denote by s_I, s_Q, d_I, d_Q. The model for the data is:

$$s_I = \alpha_1 \cos(\phi_1) + \alpha_2 \cos(\phi_2) + n_{sI}$$
$$s_Q = \alpha_1 \sin(\phi_1) + \alpha_2 \sin(\phi_2) + n_{sQ}$$
$$d_I = \alpha_1 \eta_1 \cos(\phi_1) + \alpha_2 \eta_2 \cos(\phi_2) + n_{dI}$$
$$d_Q = \alpha_1 \eta_1 \sin(\phi_1) + \alpha_2 \eta_2 \sin(\phi_2) + n_{dQ}$$

where

$$\alpha_i = \sqrt{\kappa} A_i G_\Sigma^2(\theta_i) p_0$$
$$\eta_i = \frac{G_\Delta(\theta_i)}{G_\Sigma(\theta_i)} = \text{DOA for Target } i$$

κ = constant proportional to the transmitted power

p_0 = matched filter gain

A_i = amplitude of target i

ϕ_i = phase of the return of signal of target i

θ_i = off-boresight angle of Target i

$G_\Sigma(\theta)$ = sum channel antenna voltage gain at the angle θ

$G_\Delta(\theta)$ = difference channel antenna voltage gain at the angle θ

and

$$n_{sI} \sim N(0, \sigma_s^2)$$
$$n_{sQ} \sim N(0, \sigma_s^2)$$
$$n_{dI} \sim N(0, \sigma_d^2)$$
$$n_{dQ} \sim N(0, \sigma_d^2)$$

The notation $N(a, b^2)$ indicates a normal distribution with mean a and variance b^2. The processing described below treats the quantities $\kappa, p_0, G_\Sigma(\theta), G_\Delta(\theta), \sigma_S^2, \sigma_D^2$ as known. In addition, we make three assumptions:

1) The noise contributions ($n_{sI}, n_{sQ}, n_{dI}, n_{dQ}$) are independent.
2) The target amplitudes (A_1, A_2) are Rayleigh distributed with parameters A_{10}, A_{20} known in the processor, and in additions are independent form pulse to pulse.
3) The ϕ's are uniformly distributed in $[0, 2\pi]$ and are also pulse-to-pulse independent.

Assumption 2) differs from the assumption in [3] about the target strength. In [3] the ratio of the two target strengths is known but the absolute levels are unknown. Dealing with an unknown target strength arises in most real-world tracking and detection problems. One way to handle it within the likelihood framework is to posit a probability distribution over the unknown quantity, and then to form the likelihood function by integrating over this distribution. This point is discussed further in Section 6.3 of [6].

3. Statistics of the Monopulse Ratio

In order to correctly incorporate the measurement information and fuse the pieces together UDF uses likelihood functions. A likelihood function is the conditional probability of the measurement given the target state. In a particular problem, the new work to be done is computing the measurement likelihood functions. This usually means understanding the statistics of the data either through extensive data analysis, or preferable through physics.

The monopulse ratio *y* is in complex notation

$$y_I = \mathrm{Re}\left| \frac{d}{s} \right| = \frac{d_I s_I + d_Q s_Q}{s_I^2 + s_Q^2}$$

$$y_Q = \mathrm{Im}\left(\frac{d}{s} \right) = \frac{d_Q s_I - d_I s_Q}{s_I^2 + s_Q^2}$$

The standard single-target monopulse processor takes y_I as an estimate of the DOA of the target and converts this DOA back to an angle off boresight using the relation between DOA and the beam patterns.

Following reference [2], let

$$s_I = \Lambda \cos(\psi) \quad s_Q = \Lambda \sin(\psi)$$

be the decomposition of the complex sum signal into its amplitude and phase. Define

$$R_1 = \frac{\alpha_{10}^2}{\sigma_s^2} \quad \text{and} \quad R_2 = \frac{\alpha_{20}^2}{\sigma_s^2}$$

to be the SNRs for the two targets, and

$$R_o = \frac{\Lambda^2}{2\sigma_s^2}$$

the "observed SNR."

The joint distribution of y_I and y_Q is computed in [2] as a function of joint target state. They show that conditioned on the received amplitude in the sum channel the two variables are independent and Gaussian. The parameters for the Gaussian distribution are

$$f(y_I|\Lambda,\Phi) = N\left| \frac{R_1\eta_1 + R_2\eta_2}{R_1 + R_2 + 1}, \sigma_1^2 \right|$$

$$f(y_Q|\Lambda,\Phi) = N(0, \sigma_1^2)$$

$$f(R_o|\Phi) = \frac{1}{R_1 + R_2 + 1} \exp\left(-\frac{R_o}{R_1 + R_2 + 1} \right)$$

where

$$\sigma_1^2 = \frac{q}{2R_o}$$

$$q = \left| \frac{\sigma_d^2}{\sigma_s^2} + \frac{R_1\eta_1^2 + R_2\eta_2^2 + R_1R_2(\eta_1 - \eta_2)^2}{R_1 + R_2 + 1} \right|$$

and Φ stands for the set $\{\alpha_{10}, \alpha_{20}, \eta_1, \eta_2, \sigma_S, \sigma_D\}$ of parameters. These equations will be used as the likelihood functions described below.

4. Application of Unified Data Fusion

In this section we describe the particular implementation of UDF used in the examples to follow. The implementation uses a discrete form for the state space. The UDF theory allows a continuous probability density, but the discrete form has shown to be beneficial and practical with other tracking problems.

4.1. State Space

The state space *S* for a single target is two-dimensional: position and velocity. In addition, we append a state denoted ϕ to represent the condition that the target is not currently in the surveillance region. We will use 69 position cells and 3 velocity cells, so the extended state space S^+ is

$$S^+ = \{1,2,\ldots,69\} \times \{-1,0,+1\} \cup \{*\}$$

The choice of 69 position cells was made to facilitate conversion from cell units to beamwidth units for this example. The non-zero velocity states represent targets moving one cell per time interval in either direction.

The joint state space of the two targets is

$$\mathbf{S}^+ = S^+ \times S^+$$

The joint state space is the union of four components representing the possibilities of two targets present, no targets present, or one or the other targets present. This decomposition will be evident in the computer displays described below. The joint state space has 42,849 cells.

4.2. Likelihood Function

Given the data from a number of pulses, we need to compute the conditional probability that the data was produced by a particular target state. In general, we have the following definition:

$$L_k(y_k|\mathbf{s}) \equiv \Pr\left\{Y_k = y_k \middle| \mathbf{X}(t_k) = \mathbf{s}\right\}$$

where Y_k is the random variable representing the observation at time t_k, and **s** is a joint target state in the space $\mathbf{S}^+$ defined above.

We can directly use the probability functions described in the previous section to compute the likelihood function. For each point in the state space we use the following procedure. Let *M* be the number of pulses in the dwell. Let $\overline{R}_i$ be the SNR of the *i*th target on the radar axis; these quantities are assumed known in the processor. Let

$$R_i = \overline{R}_i\, G_\Sigma^4(\theta_i) \text{ for } i = 1,2$$

This is the SNR of the *i*th target as a function of position in the beam. The target's SNR decreases as it moves away from the radar axis. For $j = 1,\ldots,M$ let

$y_I(j) =$ real part of the monopulse ratio for the *j*th pulse

$y_Q(j) =$ imaginary part of the monopulse ratio for the *j*th pulse

$R_o(j) =$ observed *SNR* for the *j*th pulse

and also let

$$\mathbf{y_I} = (y_I(1),\ldots,y_I(M))$$

$$\mathbf{y_Q} = (y_Q(1),\ldots,y_Q(M))$$

$$\mathbf{R_o} = (R_o(1),\ldots,R_o(M))$$

Define

$$\eta_i = \frac{G_\Delta(\theta_i)}{G_\Sigma(\theta_i)}$$

$$\mu = \frac{R_1\eta_1 + R_2\eta_2}{R_1 + R_2 + 1}$$

$$q = \left| \frac{\sigma_d^2}{\sigma_s^2} + \frac{R_1\eta_1^2 + R_2\eta_2^2 + R_1R_2(\eta_1 - \eta_2)^2}{R_1 + R_2 + 1} \right|$$

and for $j = 1, \ldots, M$

$$\sigma_1^2(j) = \frac{q}{2R_o(j)}$$

Then, with these definitions we have the likelihood function

$$L\left(\mathbf{y_I}, \mathbf{y_Q}, \mathbf{R_o} \middle| (x_1, x_2)\right) =$$

$$\prod_{j=1}^{M} \frac{1}{\sqrt{2\pi\sigma_1^2(j)}} \exp\left| -\frac{(y_I(j) - \mu)^2}{2\sigma_1^2(j)} \right| \frac{1}{\sqrt{2\pi\sigma_1^2(j)}} \exp\left(-\frac{y_Q^2(j)}{2\sigma_1^2(j)} \right) \frac{1}{R_1 + R_2 + 1} \exp\left(-\frac{R_o(j)}{R_1 + R_2 + 1} \right)$$

Throughout this discussion, θ_i is the angle off the radar axis for single target state x_i, and if a target is not in the sum beam, then we set the DOA and SNR of that target to 0.

4.3. Beam Pattern

For the simulation results presented we have used a cosine-squared antenna pattern

$$G_\Sigma(\theta) = \cos^2(1.1437\theta)$$

which [5, pg. 140] shows to be a good approximation to the idealized squinted-sinc pattern. The difference pattern is

$$G_\Delta(\theta) = \frac{1}{\sqrt{2}} \sin(2.2874\theta)$$

Figure 1 shows the two squinted beams used to produce this pattern, while Figure 2 shows the sum and difference patterns. The normalized error signal which relates the angle off boresight to the DOA is

$$\eta(\theta) = \sqrt{2}\tan(1.1437\theta) \approx 1.61746\theta$$

This is shown in Figure 3.

We normalize the off-boresight angle by the FWHM of the one-way voltage pattern in the sum channel. The “target present” part of the state space is taken to be between the first nulls of the beam pattern to the left and right of boresight; this is ±1.373 beamwidths. As noted above, we have used 69 spatial cells for this interval, so each cell is approximately 4% of the beamwidth.

Figure 1. Squinted Beam Patterns

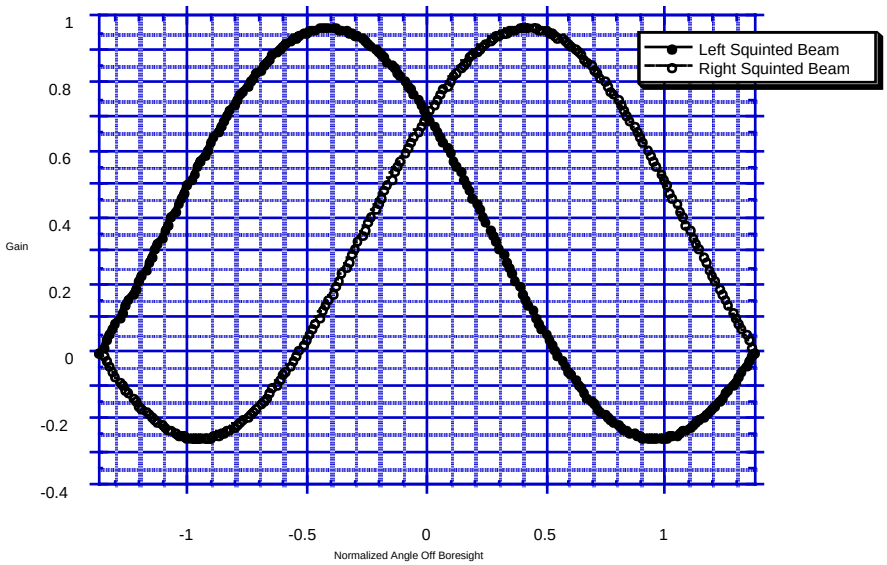

4.4 Motion Model

The motion model describes our assumptions about the probability of a specific target track through state space. The model is used to propagate probability mass between information updates. It provides the “time integration” of the measurement likelihood functions. For the simulation we assume that the targets move independently of each other. The motion for each target is also assumed to be a Markov process, which permits a recursive updating of the

Figure 2. One-way Voltage Sum and Difference Patterns

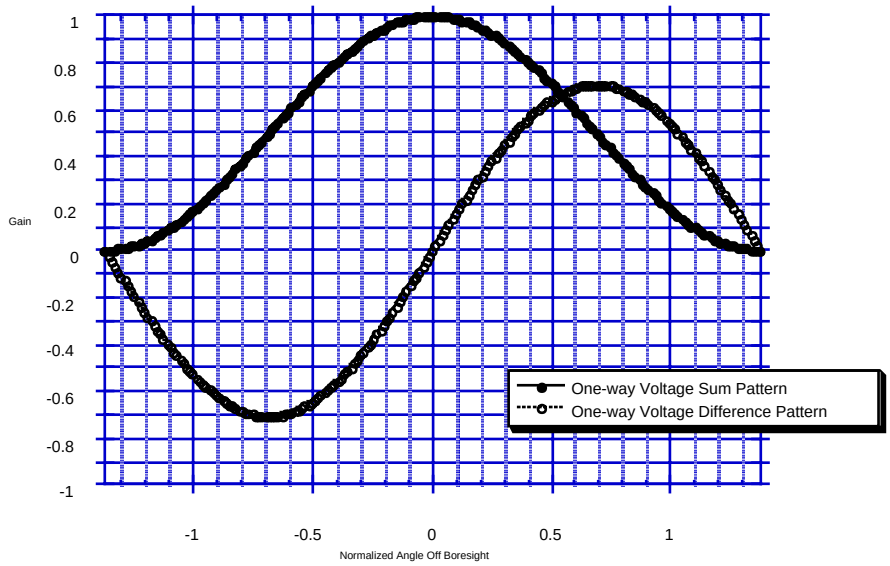

Figure 3. Normalized Error Signal

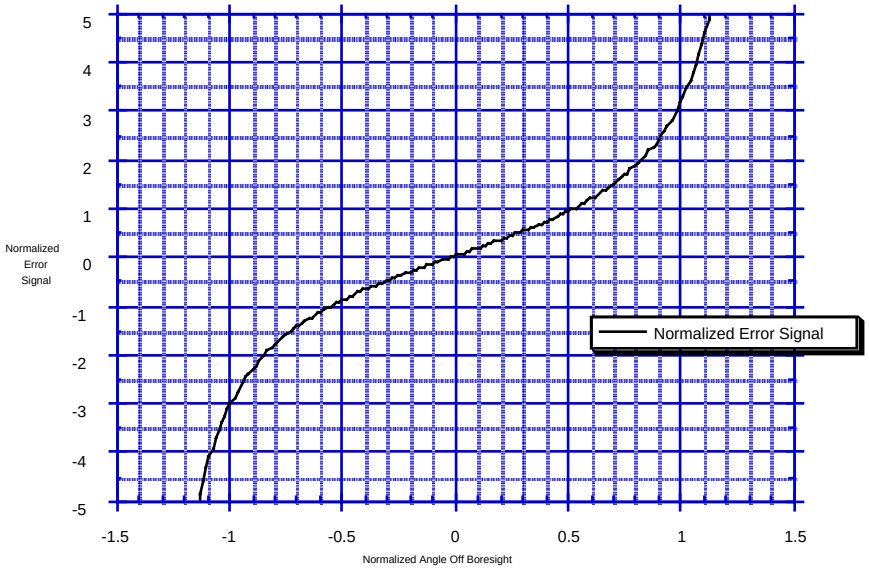

probability density (see [6]). Specifically, each target will change its velocity with probability 5% per time step to one of the other two velocities. If the motion takes the target out of the surveillance region, it has moved into state ϕ. Once a target is in state ϕ, it can reenter the surveillance region from either side of the state space. We assume that in any time step the probability of reappearing is 2%.

Alternate motion models are possible in the UDF framework. The two targets do not have to move independently; if from a joint state they are more likely to move to another joint state (in a formation, for example) that can easily be accommodated. One interesting alternative motion model is relevant for the unresolved target problem considered here. One way that two closely spaced "targets" may arise is from a primary target ejecting a decoy, either a noisemaker in a sonar example or some chaff in a radar example. The motion model for such behavior would be to assign a probability of transitioning from a single target present state in the joint state space—say $(x,v)\times\phi$—to a state with two targets present at the same spatial location—$(x,v)\times(x,v')$—with a certain probability. Tracking with this motion model may allow a missile or torpedo to maintain track on the primary target even after the decoy is ejected.

5. Sample Likelihood Functions

In this section we show examples of the measurement likelihood function in four cases for a range of parameters.

5.1 Example 1—Two 20 dB Targets

Both targets are in the sum beam, each one quarter beamwidth off of the axis. The SNR of each target is 20 dB and the dwell consists of 6 pulses. Figure 4 shows three examples of the measurement likelihood with simulated data. The first target's position is plotted along the *x*-axis and the second target's along the *y*-axis. The gray square is the true pair location and the white square is the conjugate point, where the target locations have been interchanged. Ticks along the axes are at one-half beamwidth intervals. Each likelihood function is symmetric about the $y = x$ line since the targets are indistinguishable. If the targets had different target strengths (real or assumed) then the figures would no longer be symmetric.

The first panel shows a fairly well-behaved likelihood function. The peak of the likelihood function is near the true pair location. There is negligible support (appearing as white in the display) to the hypotheses of either one target or no targets present. This likelihood

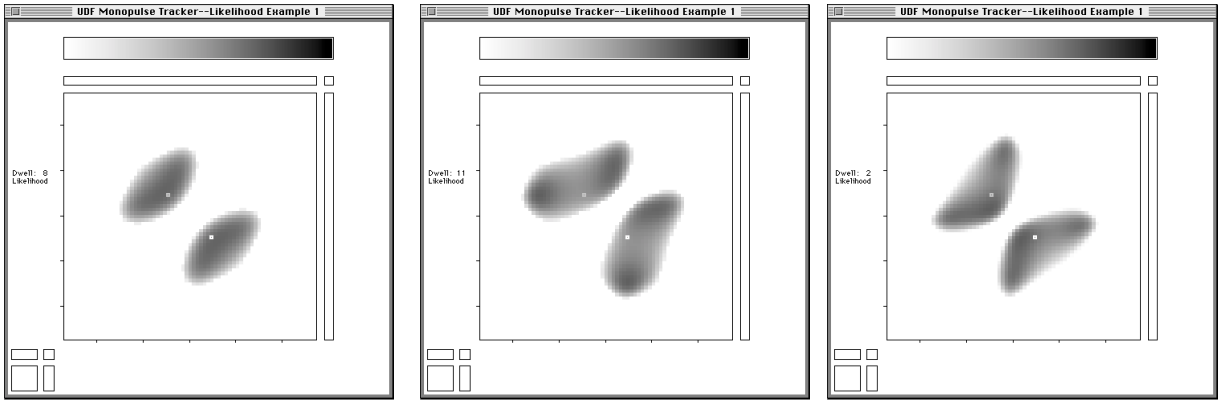

Figure 4 Sample Likelihood Functions for Two 20 dB Targets With One Half Beamwidth Separation

function could be approximated closely by a Gaussian. However, the plot shows that the measurement implies correlation between the locations of the two targets, which would be lost by treating each target independently. The second panel shows a likelihood function that is bimodal with the peaks away from the true pair location. The third panel shows a likelihood function that has a ridge-like structure along its peak making it difficult to approximate by a Gaussian.

5.2 Example 2—Two 8 dB Targets

In the second example the targets are in the same locations, but the target SNRs have decreased to 8 dB each. The results are shown in the three panels of Figure 5. The first panel shows a likelihood function with its peak near the true locations. Note however that there is some visible likelihood that the response was caused by a single target. The second panel shows the likelihood function for a second set of simulated observations. The likelihood function is very diffuse, with significant probability that there is only one target. The peak is still located in the part of state space representing two targets present. The third panel shows a third likelihood function. There is little structure to this likelihood function. The measurements can be equally plausibly explained by a number of hypothetical target locations.

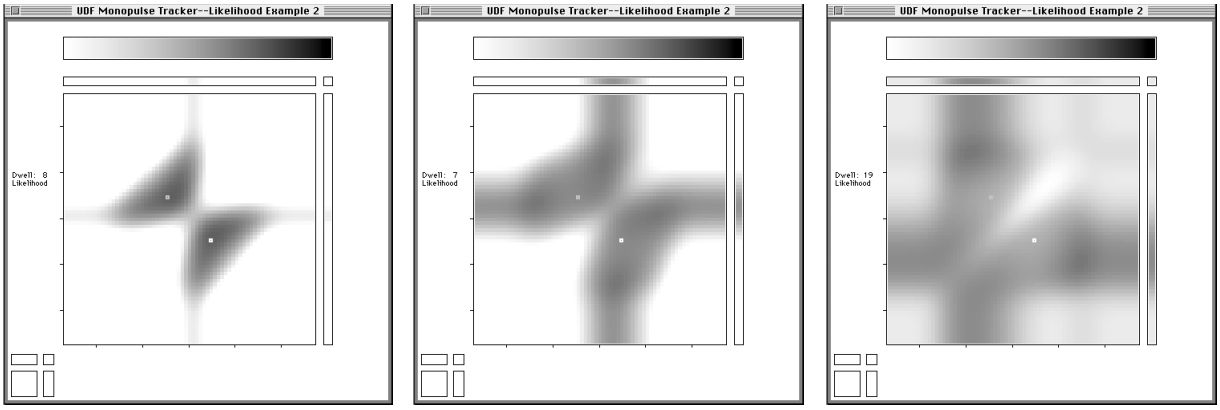

Figure 5. Sample Likelihood Functions for Two 8 dB Targets With One Half Beamwidth Separation

5.3 Example 3—One 15 dB Target

Here a single target with SNR of 15 dB is present on the axis of the sum beam. The results are shown in Figure 6. The first panel shows the true target location as the gray square in the upper rectangle. There is a very high likelihood that targets in this configuration generated the measurements. However, there are a number of other plausible explanations as well. First, there is the target interchange symmetry discussed above, so it is just as likely that target two is in the beam and target one is absent; this is the black peak in the right-hand rectangle. The longer dark streaks in the middle square represent hypotheses where both targets are present, one in the center of the beam and the other near the edge of the beam. These are also equally likely hypotheses since a target near the edge of the beam would not return much energy or greatly affect the monopulse ratio, and could be confused with noise. The last peak is in the middle of the large

square. This peak is the hypothesis that the two targets are nearly coincident at the center of the beam. The signal generated by such a configuration would look like a 3 dB stronger version of a single target. The slightly reduced likelihood at that configuration is due to the fact that the measurements are not quite that strong. The second panel shows a similar picture, but with a bit more uncertainty.

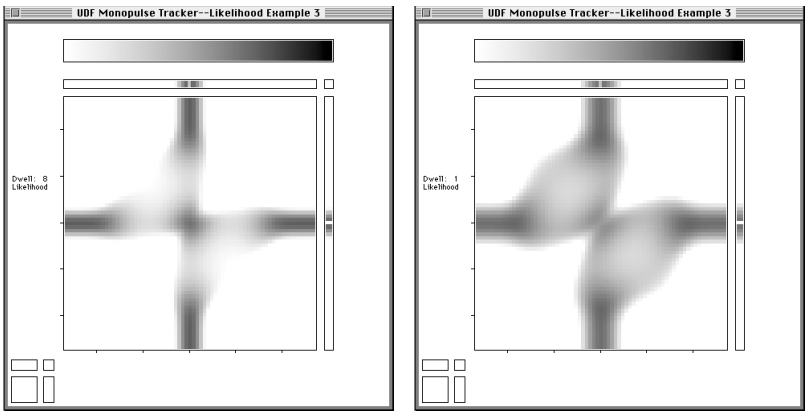

Figure 6. Sample Likelihood Functions for a Single 15 dB Target On the Radar Axis

5.4 Example 4—Noise Only

The final likelihood example examines the noise-only case with an assumed target strength of 15 dB. The results are shown in Figure 7. The likelihood function has a high value in the upper-right square which corresponds to the hypothesis of both targets not present. There is also significant likelihood in the single target components and the double target component. However, in each of those cases if a target is present the data indicates that the target must be near the edge of the beam. With our model the data supports any of those hypotheses.

There are many variations on the examples above that have been investigated, including targets with different strengths. By considering the joint state space, the UDF tracker can simultaneously treat cases with two, one, or no targets, and the transition between cases.

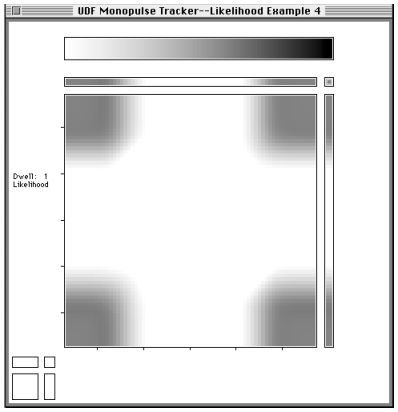

Figure 7. Sample Likelihood Function for a Case With No Targets Present

6. Tracking Example

The final example shows a complete tracking scenario. The two targets start at the edges of the main beam, target one from the left and target two from the right. Each target will move across the beam at a constant velocity of one spatial cell per time period for a total of 69 time steps. The SNR of each target is 8 dB, the same as the second likelihood example in the previous section. The initial probability distribution is 10% that each target is present. This initial probability is uniformly distributed over the 69 cells. The two targets are independent initially. The motion model was described in Section 4.4. We have simulated a sequence of observation, run the UDF tracker, and captured the likelihood function and posterior distribution every five time steps. A subset of those results is shown in Figures 8-11.

In Figure 8 we see a likelihood function similar to the one with no targets present in the previous section. It is not as well defined since the UDF tracker is looking for weaker targets (8 dB here vs. 15 dB above). The posterior distribution on the right is obtained by multiplying the prior by the likelihood. There is 89.8% probability that there are no targets present, 5.0% probability that target one only is present, 5.0% chance that target two only is present, and 0.2% chance that both are present. These numbers can be seen near the bottom left of the posterior display. The posterior distribution after only one measurement largely reflects the initial distribution. After 10 measurements (not shown), the picture is only slightly altered. The probability of a target being in the beam increases due to the motion model which allows a target to enter, and that motion is not contradicted by the measurements which allow a target to be near the edge of the beam.

In Figure 9 we see a likelihood function that senses a target located about 0.7 beamwidths to the right. It could be either target, or it could be the pair. The posterior distribution shows significant probability (35.4%) that target one is present and an equal amount that target two is

present. In either case, if that target is present the location is about 0.7 beamwidths to the right of the axis.

In Figure 10 we see that both targets have been localized quite well. The only tenable hypothesis is that there are two targets present (shown as 100.0% to the precision of the displays). This was brought about by fusing five likelihood functions for measurements 16-20 similar to the likelihood shown on the left of Figure 10. Also note in the right panel of Figure 10 the velocity marginals in the lower left. We see that the mass is concentrated on the true velocity hypotheses on target one moving right and target two moving left. The second peak is related to the conjugate hypothesis where the targets are interchanged.

As the targets approach in Figure 11, we see that the likelihood functions have high values on hypotheses with one target present at the center of the beam. These however do not alter the state distribution since they are not linked in time to any credible target track: for the last few time steps we were sure that the two targets were in the beam and approaching the axis; one could not just disappear in our model. As the targets approach, the posterior distributions lose their roundness and become wedge shaped, reflecting the structure of the likelihood functions near passage.

As the targets separate, we have similar likelihood functions in reverse order. The posterior stays very well localized on the true target location as the targets are in the main part of the beam. As the targets move to the edge, the likelihood functions give less precise information, and the diffusion in the motion model comes into play.

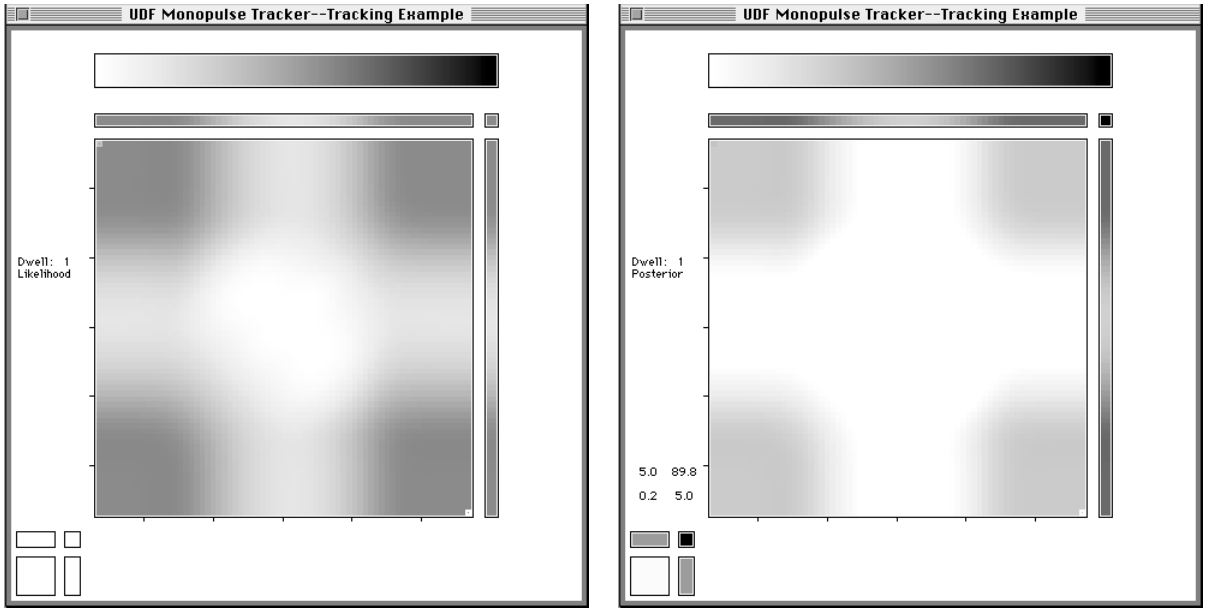

Figure 8. Likelihood and Posterior Distribution After Measurement 1

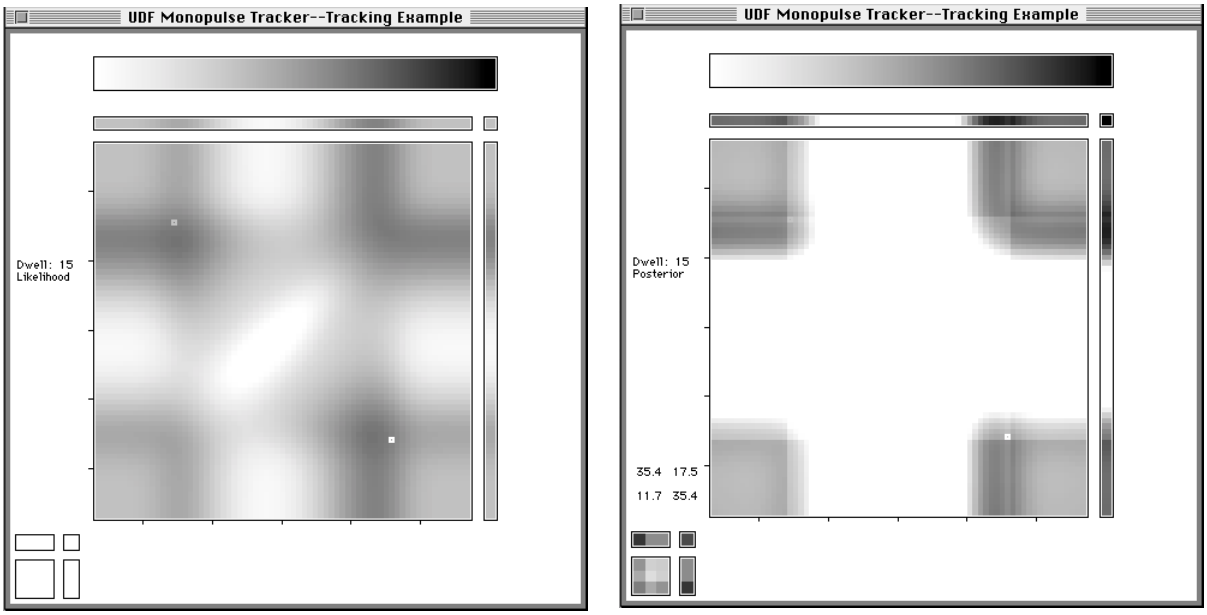

Figure 9. Likelihood and Posterior Distribution After Measurement 15

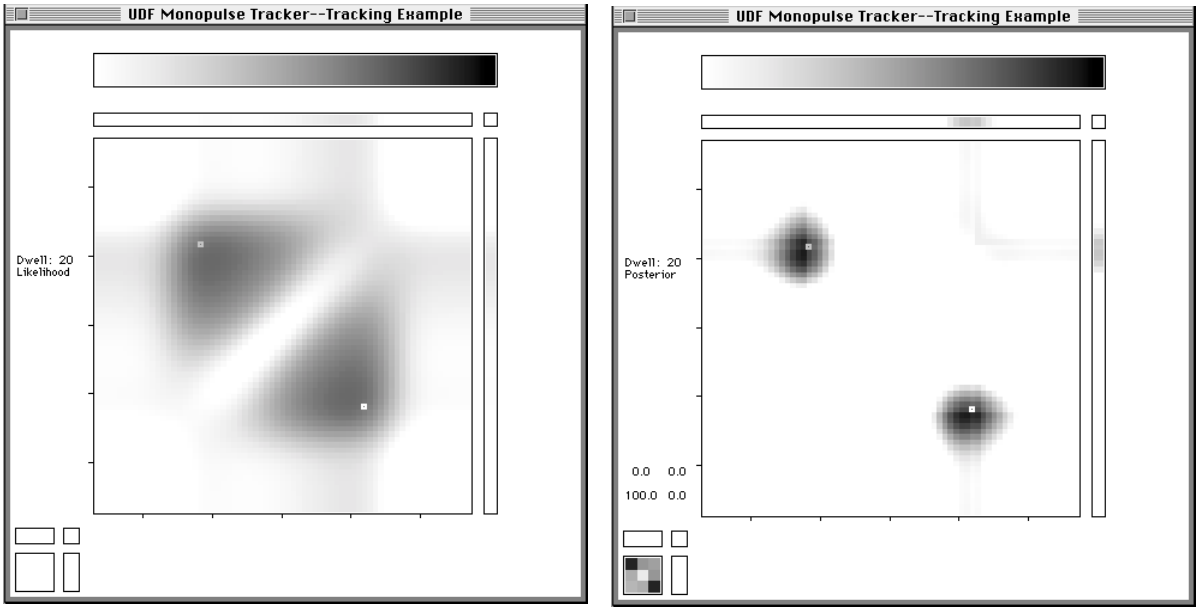

Figure 10. Likelihood and Posterior Distribution After Measurement 20

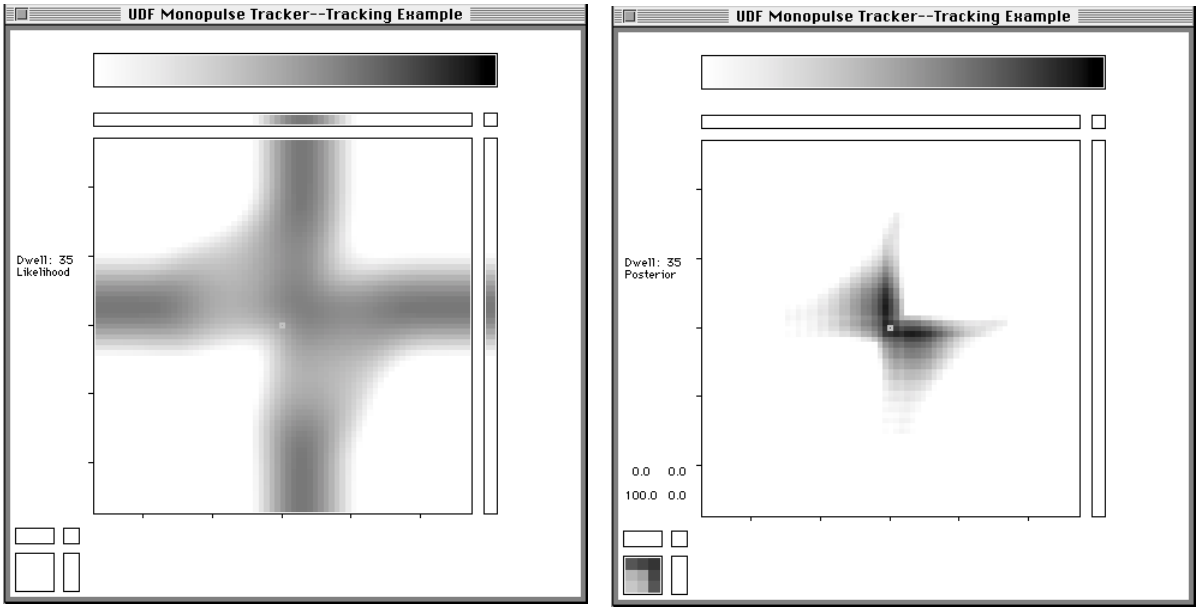

Figure 11. Likelihood and Posterior Distribution After Measurement 35

7. Summary

The examples in this paper show that the problem of tracking unresolved targets by a monopulse radar is a natural application for Metron's Unified Theory of Data Fusion. UDF handles the full generality of beam pattern, motion model, nonlinear dynamics, and a variable number of targets. In the examples shown, the target strength was known to the processor. A tracking scenario was shown where two 8 dB targets moved from one side of the beam to another, crossing in the middle. After the targets were 0.75 beamwidths off the radar axis, the posterior distribution was well localized around the true target location. The bias problem described in [3] did not appear.

Acknowledgments

The general theory of Unified Data Fusion used in this paper was developed in collaboration with Lawrence D. Stone and Carl A. Barlow of Metron. The sponsor at the Office of Naval Research was Dr. David H. Johnson.

References

[1] Barlow, C. A., Stone, L. D., and Finn, M. V. "Unified Data Fusion," in *Proceedings of the 9th National Symposium on Sensor Fusion*, vol. 1, 12-14 March 1996, pp. 321-330.

[2] Blair, W. D. and Brandt-Pearce, M. "Statistical Description of Monopulse Parameters for Tracking Rayleigh Targets," *IEEE Trans. Aerospace and Electronic Systems*, Vol. 34, No. 2, April 1998, pp. 597-611.

[3] Blair, W. D., Watson, G. A., and Brandt-Pearce, M. "Monopulse Processing for DOA Estimation of Two Unresolved Rayleigh Targets With Known Relative RCS," *29th IEEE Southeastern Symposium on System Theory*, Cookeville, TN, March 1997.

[4] Roberts, C. A. and Favret, A. G., "Application of Monopulse Tracking Techniques to Passive Linear Arrays," *Journal of the Acoustical Society of America*, Vol. 51, No. 1 (Part 1), January 1972, pp. 31-37.

[5] Sherman, Samuel M. *Monopulse Principles and Techniques*, Artech House, Dedham, MA, 1984.

[6] Stone, Lawrence D., Barlow, Carl A, and Corwin, Thomas L. *Bayesian Multiple Target Tracking*, Artech House, Dedham, MA, 1999.